PHYSOR-2006, ANS Topical Meeting on Reactor Physics
Organized and hosted by the Canadian Nuclear Society. Vancouver, BC, Canada. 2006 September 10-14

The Implementation of a 3D Characteristics Solver for the Generation of Incremental Cross Sections for Reactivity Devices in a CANDU Reactor

Romain Le Tellier*, Alain Hébert and Guy Marleau
École Polytechnique de Montréal
C.P. 6079 succ. "Centre-Ville"
Montréal Qc. CANADA H3C 3A7

Abstract

We are presenting issues related to the generation of consistent incremental cross sections for the reactivity devices in a CANDU reactor. Such calculations involve the solution of the neutron transport equation over complex 3D geometries representing a single vertical reactivity device inserted mid-way between two horizontal fuel channels. The DRAGON lattice code has recently been upgraded and can handle the exact geometry of such configurations for trajectory-based transport solvers. Within this framework, the detailed representation of the reactivity devices implies an increase in the number of regions when the strongly absorbing regions and fuel clusters are described without cylinderization. In this paper, a solution based on the characteristics method is compared with the standard procedure, based on the collision probabilities method. The coherence of both solvers is highlighted and a comparison of their computational costs is presented.

KEYWORDS: CANDU, incremental cross sections, method of characteristics, 3D geometry

1. Introduction

In the context of a CANDU reactor, so-called 3D supercell calculations are required to model the reactivity devices perpendicular to the horizontal fuel channels [1]. Such a calculation consists in fact in three transport computations performed on a geometry consisting in a device surrounded by two fuel bundles. In the reference case (referred to as the "unrodded" case), the whole reactivity mechanism is replaced by heavy water whereas the two other cases correspond to the mechanism in its two extreme configurations. For an adjuster, this means a first calculation with the rod fully extracted and a second one with the rod fully inserted within the assembly. In the case of liquid zone controllers (LZC), the two calculations correspond to a 0% and a 100% light-water filling of the controller. For each calculation, the macroscopic cross sections are homogenized over the whole geometry and are condensed into a typical two-group structure. The incremental cross sections $\Delta\Sigma$ for the reactivity device are then computed as the difference between the cell averaged cross sections obtained from the last two calculations

*Corresponding author, E-mail: romain.le-tellier@polymtl.ca

(100% filled and voided LZC). In core calculations, the effect of these devices is taken into account by adding these incremental cross sections to the cross sections of the homogenized cell.

Up until now, 3D assemblies of cluster geometries could not be represented with the standard EXCELT tracking module of the DRAGON lattice code [2]. Consequently, as presented in Ref. 1, the standard procedure for the generation of incremental cross sections involves a simplified 3D annular model for the fuel bundle and the LZC. The recent introduction of the NXT tracking module [3] has enlarged the geometrical handling capabilities of DRAGON and it is now possible to treat the LZC in their exact 3D supercell geometry.

This paper focus on the first results using an exact geometry for the generation of incremental cross sections. It is limited to LZC calculations which effectively involve the most complex geometry. In Ref. 4, the method of characteristics (MOC) was used for incremental cross sections calculations in the standard procedure. As the number of regions with this modeling is small (about 40), it was found slower than the CP method. With these new geometries, a greater number of computational regions is introduced and we are interested in evaluating the performances of a computational scheme based on a MOC solver.

The method of characteristics has been the subject of important investigations at École Polytechnique de Montréal [5–8]. This approach has the capability to be used for full-core calculations, provided that some issues related to data parallelization are correctly taken into account [9]. The method of characteristics can also be used as a transport solver in the self-shielding, leakage and multigroup flux solution components of the lattice code [10].

We present here a custom implementation of a characteristics approach that uses the algebraic collapsing acceleration (ACA) proposed by Suslov in the code MCCG3D [11]. These capabilities are available in a development version of the DRAGON code [3]. This approach will be compared with the standard procedure, based on collision probabilities actually used to perform such calculations.

The NXT tracking procedure is described in Sect. 2. and the implementation details of the proposed characteristics method are given in Sect. 3. The LZC modeling for a CANDU-6 reactor is presented in Sect. 4. and numerical results are given in Sect. 5. Our conclusions are finally presented in Sect. 6.

2. New tracking capabilities in DRAGON

The EXCELT module of the code DRAGON was originally designed in 1986 to analyze 3-D assemblies of pin cells. At that time, when memory resources were scarce and computers were notably slow, a 3-D pin cell model was judged adequate to simulate the CANDU reactivity devices with the fuel clusters and devices represented by equivalent annular models. The main feature of the EXCELT tracking module developed in that period is that it uses a global description of the geometry where the Cartesian mesh and cylindrical regions must extend through the complete geometry. In fact, even if EXCELT has seen a large number of improvements over the years, these were always limited by the fact that a global description of the geometry was assumed. With the advent of new reactor geometries that are more and more complex and where a selective discretization of the assembly is required, it was felt that a tracking method based on a block-by-block description of the geometry was required. This lead to the creation of the NXT tracking module that was introduced in the release 3.05 of DRAGON. This module can analyze 2-D and 3-D assemblies of pin cells and CANDU clusters with a non-uniform mesh.

This NXT tracking module is based on a 3 level hierarchical description of the geometry. On

the first level one finds a Cartesian mesh. The second level is described in terms of Cartesian pin cells with x, y or z directed cylinders. Finally the third level consists in cylindrical clusters (parallel to the pin cell) which may be introduced anywhere in the pin cell. The clusters do not necessarily extend the full length of the pin cell and may be terminated by an annular region similar to that found at the end of the CANDU fuel bundles. The NXT module can use angular (EQ_n with $n \leq 16$) [12] and spatial quadratures similar to those implemented in the EXCELT module. In addition, we introduced two more angular quadrature method that were proposed respectively by Longoni in Ref. 13 and Sanchez in Ref. 14 in such a way that the angular quadrature order can now reach a value of $n = 44$. Finally, the tracking information generated by the NXT module is compatible with that provided by EXCELT. As a result, the implementation of this new module is transparent for the collision probabilities and flux solution module of DRAGON.

3. MOC Implementation Details

Our implementation of the characteristics method differs from MCCG3D in many ways. First, we use a real 3D representation of the lattice geometry, as opposed to the MCCG3D prismatic geometry. Other differences are related to the iterative strategy.

Within a region i, the scalar flux Φ_i is decomposed into two contributions, one from the incoming fluxes at the region boundary, the other from the internal source Q_i. At each iteration of the characteristics method, when the integration along the tracking lines takes place, only the former contributions are cumulatively computed, the source term being added only at the end of the sweep. Indeed, this contribution can be expressed as $p_{ii}Q_i$ in the case of isotropic scattering where p_{ii} is the so-called "self-collision" probability for a convex region and can be pre-computed before the flux calculation. This approach is numerically more stable and computationally less expensive than a direct approach in which the source term is summed up on the tracking for each flux integration. This decomposition is the starting point of the Self-Collision Rebalancing (SCR) technique [4] which performs a correction of the source contribution at the end of each iteration.

Another difference concerns the evaluation of the exponential contributions that is not carried out using exact exponential calls which are time consuming but linear interpolations in tables of $(1-e^{-x})/x$ are considered instead. These tables are generated using Taylor series expansion when x is below a defined threshold. This approach differs from the MCI implementation of Ref. 5 where Taylor's expansions are not used for small x.

Concerning the acceleration techniques, the ACA preconditionning method has also been improved by introducing a track merging technique [15] to build the acceleration system. A two-step algebraic collapsing process is then obtained which has the advantage of drastically reducing the time required to construct the ACA matrices while improving on average the ACA performances in terms of the reduction of the number of iterations [16]. The ACA matrices are stored in a Modified Sparse Row (MSR) format and the resolution of the corrective system is based on a BICGSTAB Krylov solver which uses an ILU0 preconditioner and a renumbering technique based on a level-set traversal approach. These methods, described in Ref. 17 and available in a library such as P_SPARSLIB [18], were implemented and adapted to the context of the ACA system for the preconditioning of both the source and multigroup iterations.

4. LZC Modeling

The fuel-bundle geometry of a CANDU-type reactor consists in a cluster geometry. For the standard CANDU-6 geometry, there are 4 rings of natural uranium pins as depicted in the 2D two-bundle geometry of Fig. 1. The LZC is also a cluster-type geometry. There exists three LZC configurations depending on the number of feeder tubes and scavenge tubes [1]:

type 32 which consists in 3 small scavenge tubes and 2 large feeders (c.f. Fig. 2),

type 21 which consists in 2 small scavenge tubes and 1 large feeder,

type 01 which consists in 1 small scavenge tube without feeder.

In the standard computational scheme, these clusters of feeder and scavenge tubes are replaced by a cylinder geometry which preserves the volume of the different material regions. With the introduction of the NXT tracking module in DRAGON, it is now possible to represent exactly the fuel and LZC clusters in a 3D calculation.

The set of calculations we are presenting in this paper were performed using the geometries described in Figs. 1 and 2. The self-shielding procedure is based on the improved Stamm'ler method as described in Ref. 19 without Livolant-Jeanpierre normalization and uses P_0 transport-corrected cross sections from the WLUP IAEA 69-group library [20]. The self-shielding calculations are performed on the 2D two-bundle geometry depicted in Fig. 1. A comparison with a self-shielding on the 3D geometry, which is considerably slower, has not shown any noticeable discrepancy. The flux calculation is then performed on the exact 3D geometry as described by its projections in Fig. 2 corresponding to the "type 32" LZC case. A 8×4 Cartesian meshes is used for the $x-y$ discretization while there are 4 meshes in the z direction. The symmetry with respect to the $x-z$ plane that passes through the middle of the fuel bundles was used for merging (automatically) the regions. We ended up with 352 regions and 224 outer surfaces. The tracking was performed using an EQ_{16} quadrature and a uniform track density of 100 tracks/cm^2 which resulted in a 9 Gbytes binary tracking file.

A complete parametric study on this geometry discretization and tracking parameters is out of the scope of this paper and has yet to be performed.

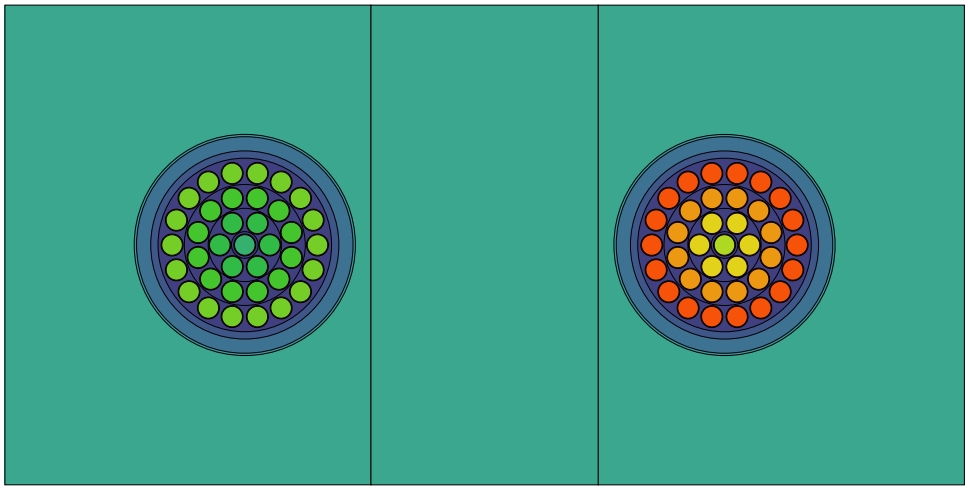

Figure 1: 2D self-shielding geometry (33 regions - 5 outer surfaces)

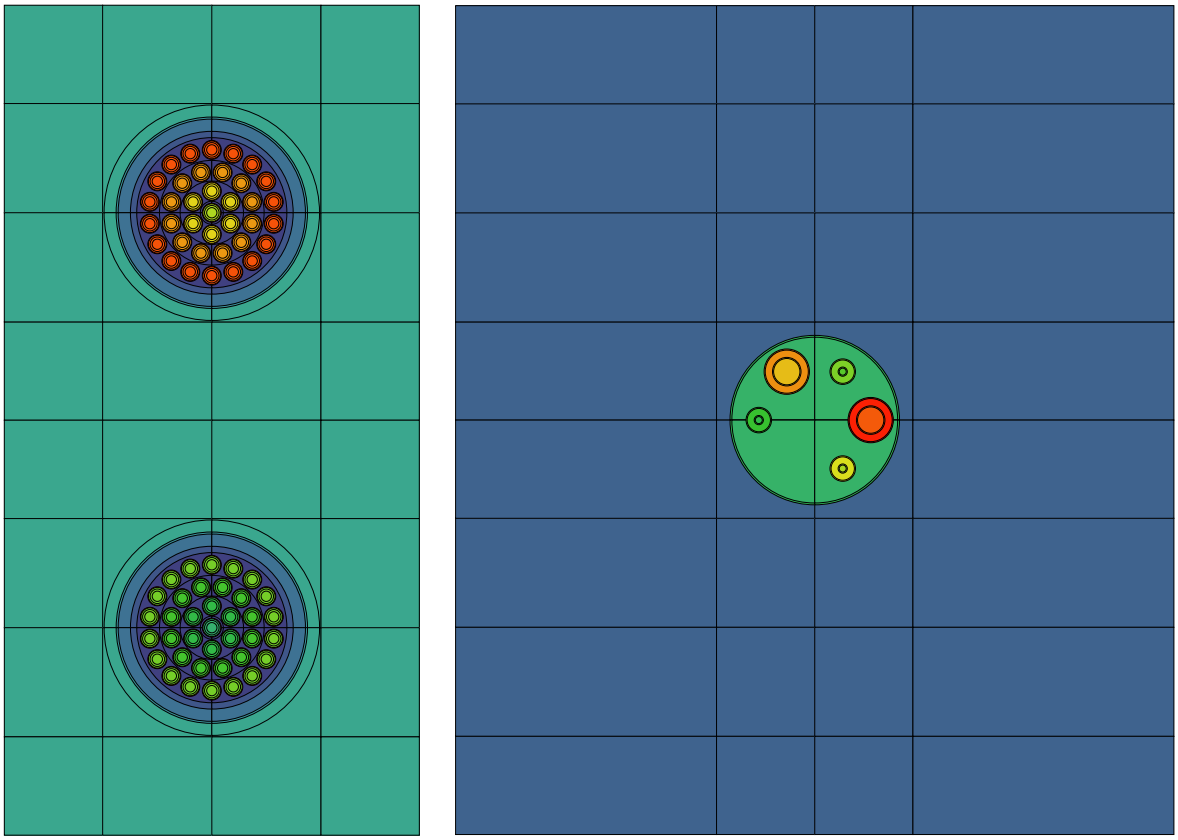

Figure 2: Projections of the 3D flux geometry

5. Numerical Results

All the calculations were performed as eigenvalue problems with white reflective boundary conditions. For the CP method, an HELIOS-type normalization [21] is used to enforce numerically the conservation laws that the collision probabilities matrix obey. The CP calculations were also performed without normalization and were found to converge to the correct eigenvalue provided that the balance enforces by the multigroup rebalancing takes explicitly into account the total leakage matrix (which is numerically not vanishing). For MOC, the neutron conservation is ensured by using surfaces evaluated numerically from the tracking file for the outer lattice boundary.

5.1 2D-3D comparison

A first set of calculations was performed in 2D on the $x-y$ projection of the 3D geometry and compared with the 3D "unrodded" calculation in order to check the coherence of the 3D modeling and the treatment of the supercell geometry. Indeed, except for the approximated boundary conditions on the $z-$ and $z+$ faces of the 3D geometry and the difference in tracking integration, the results should be very close. In Table 1, we see the coherence both between the solvers and the 2D and 3D calculations: all the k_{eff} are within 10 pcm.

Table 1: k_{eff} comparison of 2D and 3D calculations

	2D $x-y$ projected geometry	3D "unrodded" geometry
CP	1.12500	1.12492
MOC	1.12497	1.12491

5.2 LZC calculations

We present the comparison of CP and MOC solvers for the "type 32" LZC calculations. Table 2 shows the k_{eff} in the different cases for both solvers. The comparison was also carried out in terms of scalar fluxes (Φ_i^g) where $g \in [1, G = 69]$ and $i \in [1, N_r = 352]$. Their relative difference for the three configurations are presented in Table 2 in terms of

$$\epsilon_{\text{max}} = \max_{g\in[1,G]} \left(\max_{i\in[1,N_r]} \left(\frac{|\Phi_i^{g(\text{MOC})} - \Phi_i^{g(\text{CP})}|}{\Phi_i^{g(\text{CP})}} \right) \right),$$

$$\bar{\epsilon} = \max_{g\in[1,G]} \left(\frac{1}{V_{\text{tot}}} \sum_{i=1}^{N_r} \left(V_i \frac{|\Phi_i^{g(\text{MOC})} - \Phi_i^{g(\text{CP})}|}{\Phi_i^{g(\text{CP})}} \right) \right).$$

where V_i is the volume of region i and V_{tot} is the volume of the whole geometry.

Table 2: CP-MOC comparison in the different 3D configurations

	$k_{\text{eff}}^{\text{CP}}$	$k_{\text{eff}}^{\text{MOC}}$	$\bar{\epsilon}$ (%)	ϵ_{max} (%)
"Unrodded" case	1.12492	1.12491	0.076	0.34
"type 32" LZC 0%	1.09604	1.09603	0.076	0.34
"type 32" LZC 100%	0.98689	0.98691	0.076	0.36

The coherence between the solvers is clearly shown by these results. The k_{eff} are within 2 pcm and the maximum difference on the scalar flux over the spatial and energy domain is less than 0.4%. In terms of energy, this maximum difference is located in the fastest groups where the neutron flux amplitude is largely decreased.

This coherence is very interesting because it means that both solvers may be combined in a same set of calculations without introducing any discrepancy.

5.3 Computational costs comparison

For CP, the in-line tracking option was used for the integration of the collision probabilities. This approach with no tracking file creation offers a major acceleration compared to a group-per-group integration with file accesses. For MOC, a tracking file is constructed prior to the flux calculation. Then, in all the phases that requires the tracking information, the energy groups are treated in a vectorial way to limit the number of file accesses.

In terms of acceleration techniques, we compare the proposed ACA method with the SCR method proposed in Ref. 5. The SCR results are totally coherent with its original implementation in the MCI solver [15]. Note that the ACA method can also be used as a flux solver in itself to initialize the multigroup fluxes and currents; this option was also tested.

Table 3 gives the details of the MOC computational cost with these different options in comparison with the total CPU time for the CP method in the 3D "unrodded" case.

Table 3: CPU time ratio (with respect to the CP total time) in the 3D "unrodded" case

parameters		CPU time ratios			N_{outer} [a]	N_{tracking} [b]	N_{calc} [c]	Storage[d] (in kilowords)
ACA	SCR	assembly	flux	total				
-	-	0.10	8.30	8.40	24	60	4130	24.3
-	$\surd$	0.10	5.28	5.38	12	38	2622	43.4
$\surd$	-	0.37	2.78	3.15	6	20	1380	538.1
$\surd$ (init.)[e]	-	0.37	2.18	2.55	4	16	1104	538.1
CP method		1.00	0.00	1.00	5	18	1271	8549.4

[a] N_{outer} is the number of outer iterations,
[b] N_{tracking} is the number of tracking accesses,
[c] $N_{\text{calc}} = \sum_i N_g^{(i)}$ where $N_g^{(i)}$ is the number of groups processed at iteration i,
[d] Storage related to the MOC integration strategy and the SCR/ACA preconditioning,
[e] An ACA-simplified transport calculation is performed to initialize the multigroup fluxes and currents.

Is is clear from these results that MOC is not directly competitive with CP for these 3D calculations. At its best, it is about 2.55 times slower. It is important to note that our implementation of the characteristics method is slowed down by the integration strategy resulting from its Taylor's expansion treatment of vanishing optical thicknesses, a specific treatment not done in the MCI implementation of Ref. 5

However, the performances of the preconditioning techniques are well illustrated in these calculations. The ACA preconditioning offers a speed-up of about 3.29 and 2.67 with and without initialization respectively while it is about 1.56 with the SCR method. In such a case with a rather limited number of unknowns and a quite large tracking file, the time spent in solving the ACA corrective system at the end of each multigroup iteration represents less than 0.1% of the total time for the flux integration. In this context, the acceleration of the outer (power) iteration by the ACA synthetic preconditioner could be advantageous. Note that this option was retained in the original implementation of the ACA method by Suslov. This is totally different from the situation that one may encounter in 2D LWR assemblies calculations [10] where the tracking file size is much smaller while the number of unknowns is larger.

The biggest drawback of the ACA method in these 3D calculations is the time spent to build the preconditioning matrices. Even with the two-step implementation of this method, the cost of this assembly phase is still rather important, the equivalent of about 2.5 times the cost of a flux iteration with MOC. In terms of storage, for MOC with ACA, the requirement remains small, roughly 16 times smaller than for the CP solver.

It is important to note that in the context of the method of characteristics, even without the ACA initialization step, this set of three flux calculations can be speed-up by initializing the flux for the "type 32" LZC 0% (resp. "type 32" LZC 100%) calculation with the flux of the previous case i.e. the 3D "unrodded" (resp. "type 32" LZC 0%) case. It largely reduces the computational cost of this second and third calculations. For the "type 32" LZC 0% case, when

ACA is used, it gives a speed-up comparable to an ACA initialization, the number of tracking accesses is reduced from 20 to 15. This is also used with the CP method but with no substantial gain since in this case, most of the time is spent in the calculation of the collision probabilities matrices.

We have compared the performances of the CP and MOC methods within the framework of incremental cross sections calculations. Although the method of characteristics is slower than the collision probabilities method, its usage may become mandatory as the discretization is refined and the size of the problem is increased. Both methods may be used within a same study as they produced coherent results. For example, in the context of the development of the Advanced CANDU Reactor™, in Ref. 22, a parametric study for incremental cross sections that was performed on a simplified 3D geometry showed that a fine mesh along the x-axis (c.f. Fig. 2) and a fine mesh in the light water coolant are needed to obtain converged results. Consequently, with an exact description of the 3D geometry as presented in this paper, it is to be expected that an optimized characteristics method will be necessary to perform reference calculations on these discretized configurations.

6. Conclusion

With this paper, we intend to investigate the usage of the method of characteristics for the generation of incremental cross sections associated with reactivity devices in CANDU reactors. The introduction of an exact 3D representation of this geometry can produce a large number of regions as the spatial discretization is refined. Consequently, even though it is slower when the number of regions is small, the introduction of an optimized characteristics method may become necessary because of the limitation in the number of regions that can be handled with a collision probabilities formalism. As both solvers produce coherent results, they may be advantageously combined for performing this kind of analysis.

The performances of the characteristics method are greatly affected by the implementation of an adequate acceleration technique. The ACA method as presented in this paper is a good candidate to reduce the computational cost of the characteristics method on such 3D calculations. Indeed, it is efficient in reducing the spectral radius of the iterative matrix while being not too costly in terms of storage and computational resources for the resolution of the corrective system.

ACKNOWLEDGMENTS

This work was supported by grants from the Natural Science and Engineering Research Council of Canada.

References

1) R. Roy, G. Marleau, J. Tajmouati, D. Rozon, “Modelling of CANDU reactivity control devices with the lattice code DRAGON”, *Ann. Nucl. Energy*, **21**, 115-132 (1994).

2) G. Marleau, A. Hébert and R. Roy, “New computational methods used in the lattice code Dragon,” *Int. Top. Mtg. on Advances in Reactor Physics*, Charleston, March 8–11, 1992.

3) G. Marleau, A. Hébert and R. Roy, “A user’s guide for DRAGON 3.05”, *Report IGE-174 Rev. 6*, Institut de Genie Nucléaire, École Polytechnique de Montréal (2006).

™ a registered trademark of Atomic Energy of Canada Limited.

4) G. J. Wu and R. Roy, "Self-collision rebalancing technique for the MCI characteristics solver", *20th Annual Conf. of the Canadian Nuclear Society*, Montréal, 1999.

5) G. J. Wu and R. Roy, "A new characteristics algorithm for 3D transport calculations" *Ann. nucl. Energy*, **30**, 1-16 (2003).

6) R. Le Tellier and A. Hébert, "Spectral analysis of an algebraic collapsing acceleration for the characteristics method", *Int. Top. Mtg. in Mathematics & Computations, Supercomputing, Reactor Physics and Nuclear and Biological Applications. M&C 2005*, September 12–15, Avignon, 2005.

7) R. Le Tellier and A. Hébert, "Application of the characteristics method combined with advanced self shielding models to an ACR-type cell", *26th CNS Annual Conference*, June 13–15, Toronto, 2005.

8) R. Le Tellier and A. Hébert, "Application of the DSA preconditioned GMRES formalism to the method of characteristics – first results", *Int. Top. Mtg. on the Physics of Fuel Cycles and Advanced Nuclear Systems: Global Developments. PHYSOR-2004*, Chicago, April 25–29, 2004.

9) M. Dahmani and R. Roy, "Parallel solver based on the three-dimensional characteristics method: design and performance analysis", *Nucl. Sc. Eng.*, **150**, 155-169 (2005).

10) R. Le Tellier and A. Hébert, "Benchmarking of the characteristics method combined with advanced self-shielding models on BWR-MOX assemblies", this meeting.

11) I. R. Suslov, "An algebraic collapsing acceleration in long characteristics transport theory", *Proc. of the 11-th Symposium of AER*, 179-188, Csopak, September 2001.

12) B. G. Carlson, "Tables of equal weight quadrature EQn over the unit sphere", *Technical Report LA-4734*, Los Alamos Scientific Laboratory (1971).

13) G. Longoni, and A. Haghighat, "Development of new quadrature sets with the ordinate splitting technique", *Int. Top. Mtg. in Mathematics & Computations. M&C 2001*, Salt Lake City, 2001.

14) R. Sanchez, L. Mao and S. Santandrea, "Treatment of boundary conditions in trajectory-based deterministic transport methods", *Nucl. Sc. Eng.*, **140**, 23-50 (2002).

15) G. J. Wu and R. Roy, "Acceleration techniques for trajectory-based deterministic 3D transport solvers", *Ann. Nucl. Energy*, **30**, 567-583 (2003).

16) R. Le Tellier and A. Hébert, "An improved collapsing acceleration with general boundary conditions for the characteristics method", submitted to *Nucl. Sc. Eng.* in February 2004.

17) Y. Saad, "Iterative methods for sparse linear systems", *Series in Computer Science*, PWS Publishing Company, 460p. (1996).

18) Y. Saad and K. Wu, "Design of an iterative solution module for a parallel sparse matrix library (P_SPARSLIB)", *Applied Numerical Mathematics*, **19**, 343-357 (1995).

19) A. Hébert and G. Marleau, "Generalization of the Stamm'ler method for the self-shielding resonant isotopes in arbitrary geometries", *Nucl. Sc. Eng.*, **108**, 230-239 (1991).

20) D. Lopez Aldama, F. Leszczynski, A. Trkov, "WIMS-D library update - Final report of a coordinated research project", *IAEA-DOC-DRAFT*, IAEA (2003). (available on line at http://www-nds.iaea.org/wimsd/download/tecdocdraft.pdf)

21) E. A. Villarino, R. J. J. Stamm'ler, A. A. Ferri, "HELIOS: Angularly dependent collision probabilities", *Nucl. Sc. Eng.* **112**, 16-31 (1992).

22) M. Dahmani, G. Marleau, E. Varin, "Effect of burnup on ACR-700 3-D reactivity devices cross sections", this meeting.